DEVELOPMENT OF A TEST SET-UP TO MEASURE LARGE WAVE-BY-WAVE OVERTOPPING MASSES

LANDER VICTOR (1) and PETER TROCH (2)

(1) M.Sc.Eng., Ghent University, Dept. of Civil Engineering, Technologiepark 904, Zwijnaarde, B-9052, Belgium, lander.victor@ugent.be
(2) Prof., Ph.D., M.Sc.Eng., Ghent University, Dept. of Civil Engineering, Technologiepark 904, Zwijnaarde, B-9052, Belgium, peter.troch@ugent.be

Existing measurement techniques for wave overtopping are developed for sea defense structures, which give rise to small wave-by-wave overtopping masses. The development of overtopping wave energy converters however requires the identification of large overtopping masses. A new test set-up that is able to measure large wave-by-wave overtopping masses accurately is described in this paper. Starting from the weigh cell technique, a number of adaptations have been carried out, of which the effectiveness is compared in the main part of this paper. Resulting from this comparison, a final more accurate adapted test set-up is derived. Tests carried out with this test set-up reveal that the shape and scale factors of the Weibull distributions of large wave-by-wave overtopping volumes are different compared to those of the Weibull distributions corresponding to sea defense structures. The more accurate adapted test set-up can be used for all types of structures.

Keywords: Wave overtopping; large overtopping masses; wave-by-wave; measurement set-up.

1. Introduction

Traditionally, the measurement of wave overtopping in laboratory is carried out for scale models of sea defense structures. These structures are designed based on a minimization of the amount of water that overtops their crests for a specific design sea state at their locations. The amount of overtopped water is usually expressed as an average overtopping rate q, which should be limited through design to 1 - 50 l/s/m for sea defense structures in prototype, dependent on the allowed level of damage to vehicles, pedestrians, buildings,…(see e.g. CEM (2002) and EurOtop (2007)).

Overtopping wave energy converters (OWECs) - which are based on wave run-up on a slope and overtopping into a reservoir that is emptied into the sea through a set of turbines - on the other hand require a maximization of the amount of water overtopping their crests. This is achieved through a specific geometry of the slope of the OWEC in combination with a low relative crest freeboard (i.e. the vertical distance between the crest of the structure and the still water level, divided by the characteristic wave height). Figure 1 gives a definition sketch of an OWEC built in a sea defense structure. The q – values typically range from 10 l/s/m to more than 1000 l/s/m for OWECs in prototype. According to EurOtop (2007), the maximum individual volume V_{max} [l/m] for one wave equals 1000 times (for q = 1 l/s/m) to 100 times (for q = 100 l/s/m) the value of q.

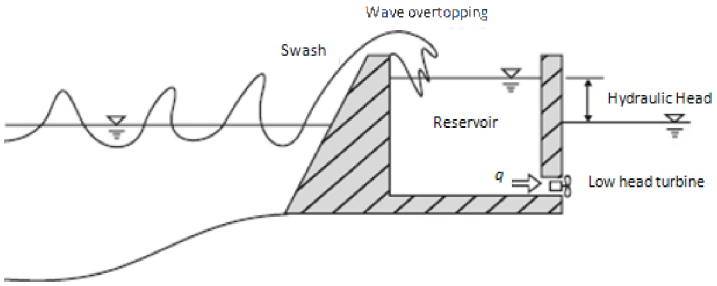

Figure 1. Definition sketch of an OWEC built in a sea defense structure (see Shin and Hong (2005))

As a consequence, much larger masses of water need to be measured for laboratory tests on OWECs compared to sea defense structures.

Moreover, the wave-by-wave overtopping masses should be measured accurately for OWECs. The reservoir of an OWEC stores the overtopped water. The water level inside the reservoir should be kept as constant as possible in order to create a buffer by the reservoir for the power output to be more constant, i.e. to improve the performance of the OWEC. The water level inside the reservoir is regulated through the turbines. Keeping a constant water level inside the reservoir requires knowledge on the water masses that enter the reservoir for every individual overtopping

wave. Those masses should be predicted for a specific OWEC geometry based on characteristics of the incident waves in front of the OWEC.

This paper discusses the development a test set-up that is able to measure large wave-by-wave overtopping masses accurately for a non-floating OWEC with a slope extending to the sea bottom, starting from a traditional overtopping measurement set-up.

2. Traditional measurement set-ups of overtopping masses

According to literature (see e.g. Kortenhaus et al. (2004a) and Troch et al. (2004)), several techniques exist to measure overtopping masses. Those techniques are primarily designed to determine the average overtopping rate q. The most widely used measurement set-ups are shown in Fig. 2.

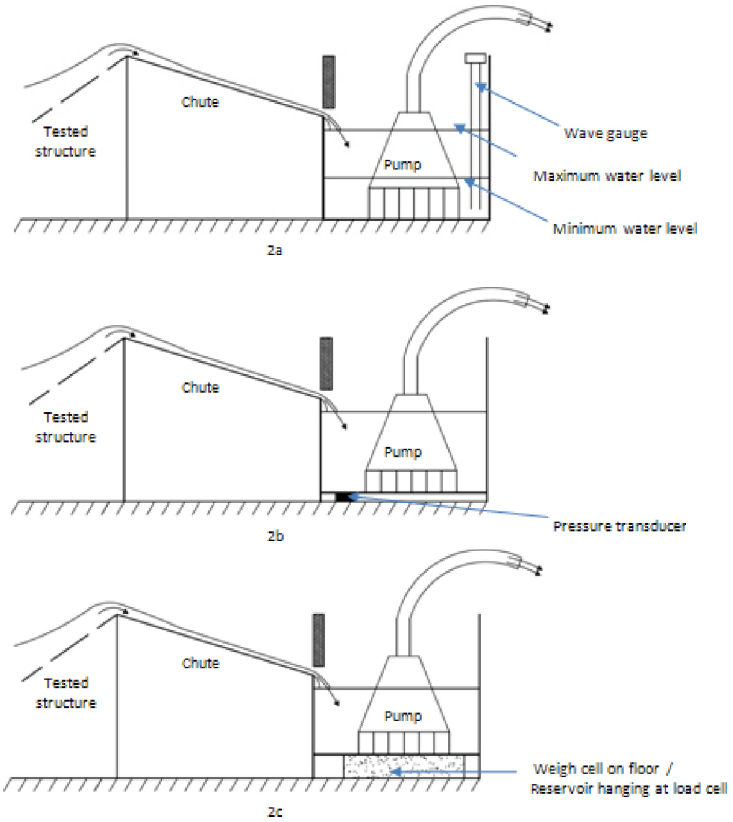

Figure 2. Most widely used techniques to measure overtopping masses

The techniques in Fig. 2 show many similarities: the overtopped water runs down a chute with a certain length down to a reservoir where the amount of overtopped water is measured continuously. All overtopping measurement set-ups require the installation of a pump inside the reservoir. The pump transports water from the reservoir to the flume in order to compensate for the decrease in water level due to the overtopped water. The allowable decrease and the expected range of q – values determine the crest width for which overtopping is measured, the size of the reservoir and the characteristics of the pump. The pump starts working for a fixed number of seconds each time a specific maximum amount of water inside the reservoir is reached.

The differences between the techniques originate from the type of measurement device that is used to determine the mass of water inside the reservoir: a wave gauge (Fig. 2a), a pressure transducer (Fig. 2b) and a weigh cell below the reservoir (Fig. 2c) or a load cell from which the reservoir is suspended. Each of these devices has its advantages and disadvantages. The wave gauge, e.g. used by Kofoed (2002) and Lykke Andersen and Burcharth (2009) for measuring overtopping masses, is an established device. However, its output signal is very susceptible to oscillations of the water level inside the reservoir, even with a covering tube made of Perspex. The size of those oscillations increases if the length of the chute decreases. Similar disadvantages are applicable for the pressure transducer, which e.g. is used for determining overtopping masses on large scale by Tedd and Kofoed (2009). In addition a pressure transducer is less easy to install. A weigh cell positioned below the reservoir is less susceptible to such oscillations due to the large dimensions of the weigh cell compared to the reservoir. Furthermore, no conversion and hence calibration of the output signal are required to read the overtopping masses. In Verhaeghe (2005), it is shown that the accuracy of small scale overtopping measurements varies in between about 10^{-6} m³/s/m for the wave gauge and pressure transducer measurement set-up and 10^{-8} m³/s/m for the weigh cell measurement set-up.

On the other hand, a weigh cell cannot be exposed to water. The weigh cell and reservoir are usually positioned outside the wave flume, requiring a long chute.

Combining the large number of advantages of the weigh cell measurement set-up leads to the development of a test set-up that is able to measure large wave-by-wave overtopping masses starting from that set-up.

3. Ability of traditional weigh cell technique to determine large wave-by-wave overtopping masses

Three different methods exist to derive the average overtopping rate based on a measured weigh cell signal. Figure 3 illustrates those three methods for an example of a small scale test with a sea defense structure (small amounts of overtopping). In the first method (Fig. 3a), q is determined from the number of times the pump works N (N = 5 in Fig. 3) and the average mass of water P that is transported during the fixed pump duration (approx. 28 kg). The expression for the average overtopping rate q is:

$$q = \text{initial mass in reservoir} - \text{mass in reservoir after test} + N \times P/\text{total time} \qquad [1]$$

Equation [1] gives a rather rough estimate for q and is only used for first estimation. A more accurate value of q is determined based on the cumulative mass of water in the reservoir (Method 2 and 3). The cumulative mass of water in the reservoir is derived from the weigh cell signal, to which a compensation for pumping is applied using the average pump characteristic. The average overtopping rate q is equal to the tangent of the average slope angle of the cumulative curve (see Fig. 3b). The same value is found by averaging the differentiated cumulative mass of water in the reservoir over time, see Fig. 3c. The large negative peaks in Fig. 3c are caused by imperfect compensation for pumping, giving rise to unrealistic descending sections of the cumulative curve in Fig. 3b. Their effect on the average differentiated cumulative mass in the reservoir over time, i.e. equal to q, is negligible. However their role is important concerning wave-by-wave overtopping masses. The identification of wave-by-wave overtopping masses can be based on the cumulative curve in Fig. 3b. Each overtopping wave will cause an abrupt increase in the curve of the cumulative mass in the reservoir over time. The differences in cumulative mass between two consequent horizontal sections of the cumulative curve in Fig. 3b correspond to individual overtopping masses, see Fig. 4. Descending sections in the cumulative curve thus lead to errors in the wave-by-wave overtopping masses.

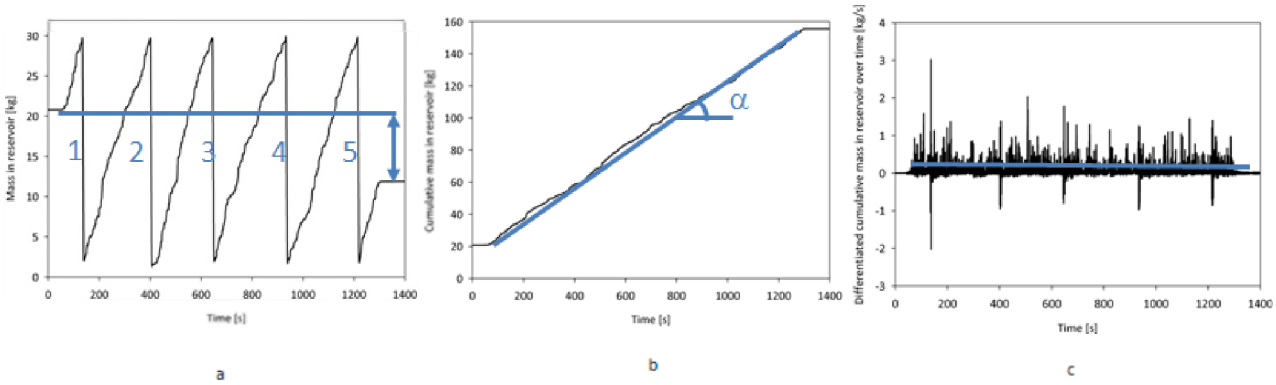

Figure 3 – Three methods to derive the average overtopping rate q for weigh cell technique

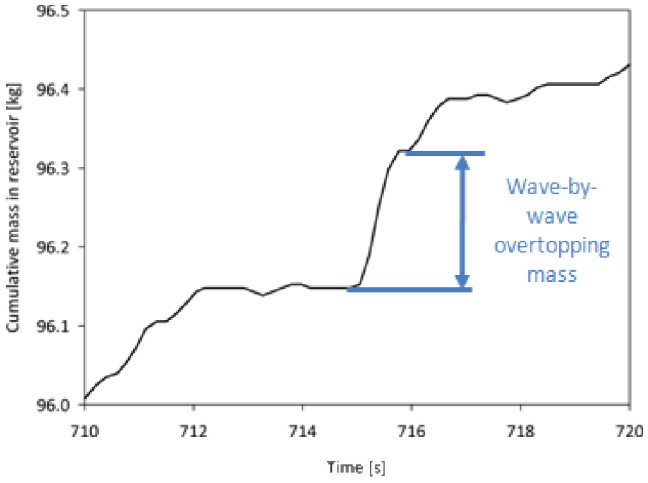

Figure 4 – Graph of cumulative mass in reservoir against time, identification of wave-by-wave overtopping masses

It is clear that a higher number of pump turns (higher N) will occur for large amounts of overtopping. In that case, an accurate compensation for pumping is even more important in order to avoid unrealistic descending sections of the cumulative curve in Fig. 3b and Fig. 4 to improve the readability of the wave-by-wave overtopping masses. Next to that, some other adaptations to the traditional measurement set-up shown in Fig. 2c should be carried out to be able to measure wave-by-wave overtopping masses accurately. A long chute, applied to obtain a dry installation of the weigh cell and reservoir outside the wave flume, causes a time delay between the moment a wave overtops the crest of the structure and the moment of registration of the corresponding water mass by the weigh cell. If two waves overtop the crest of a structure within a small time interval, the two corresponding water masses could merge along the length of the chute. Therefore, an accurate measurement of wave-by-wave overtopping masses requires a short chute.

Furthermore, identification of the wave-by-wave overtopping masses from the cumulative curve in Fig. 4 requires knowledge on the times when waves overtop the crest enabling to search for the corresponding abrupt increase in the cumulative curve. A system should be installed that identifies those times, i.e. an overtopping detection system.

The next section discusses a test set-up that takes into account the adaptations suggested above.

3. Adapted test set-up 1

A first test set-up that takes into account the adaptations mentioned above was installed in a wave flume with dimensions 25 m x 1.2 m x 1 m (length x width x height) at the Department of Civil Engineering of Aalborg University, Denmark and used for experimental tests during August – October 2008. Figure 5 shows a definition sketch (side view) of the test set-up. The reservoir and weigh cell were positioned directly behind the crest of the slope in a dry space inside the wave flume, to reduce the length of the chute. Furthermore, an overtopping detection system was installed at the crest of the slope. It consisted of two vertical wires with a limited length that are connected to a power source. The overtopping detection system operates similar compared to a wave gauge: the voltage between the two wires changes when these are covered by water. By using this property, the time when a wave overtops the crest of the structure can be identified. Finally, thorough calibrations of both reservoir and pump were carried out to accurately compensate for pumping.

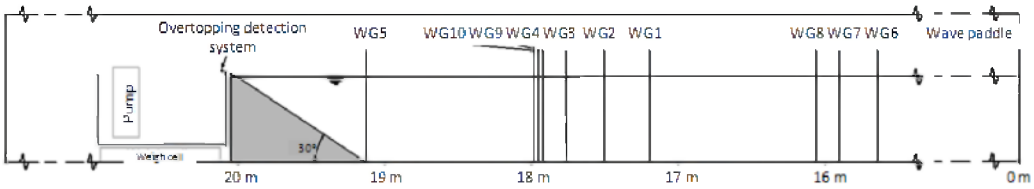

Figure 5 – Definition sketch of adapted test set-up 1

Figure 6 shows an example of a typical output of the overtopping detection signal with the corresponding weigh cell signal. The weigh cell signal is shown instead of the cumulative mass in the reservoir for visualization purposes.

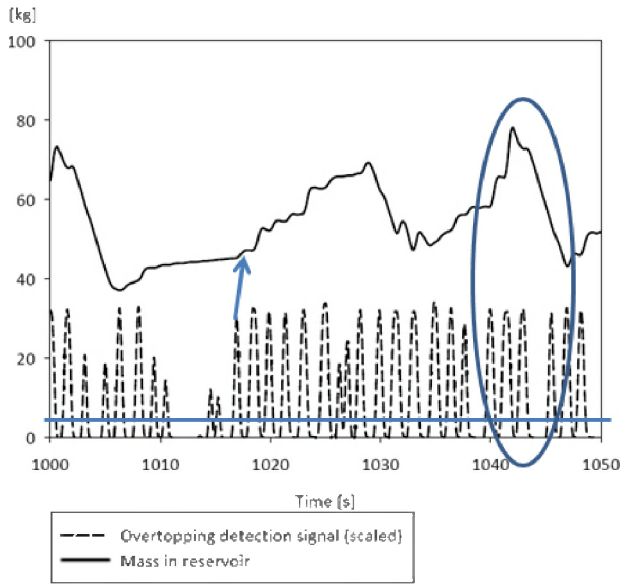

Figure 6 – Typical output of the overtopping detection system of adapted test set-up 1 with the corresponding weigh cell signal

Each peak of the overtopping detection signal in Fig. 6 that exceeds a specific threshold corresponds to a wave-by-wave overtopping mass (see arrow in Fig. 6). The maximum height of the peaks of the overtopping detection signal is limited due to the small height of the two wires compared to the overtopping flow depth of large part of the overtopping waves. This reveals one of the "children's diseases" of the first adapted test set-up. The peaks of the overtopping detection signal allow the determination of the times overtopping waves reach the crest of the slope, allowing the identification of the discrete wave-by-wave overtopping masses. The heights of the peaks are not directly related to the size of the corresponding overtopping masses, due to the limited maximum height of the peaks. It is more convenient, for setting up a prediction strategy for the wave-by-wave overtopping masses based on incident wave characteristics, convenient to link the continuously sampled wave measurements to a continuously sampled overtopping detection signal instead of to the discrete series of wave-by-wave overtopping masses. This requires an overtopping detection system that enables the identification of the wave-by-wave overtopping masses based on the size of the peaks of the overtopping detection signal.

Some other "children's diseases" appeared when carrying out the tests and when analyzing the test results. Figure 7 shows some photos of the first adapted test set-up, illustrating some of those "children's diseases". The dry area containing the reservoir and weigh cell was positioned right across the width of the flume, while the overtopped water was collected only over a crest width of 0.5 m along the centre of the wave flume. To avoid wave overtopping in the parts of the crest outside the overtopping collection zone, mild beach profiles were installed in those parts. Figure 7 shows that the resulting "slope" consisted of three zones, with a highly reflective zone in the centre, i.e. the actual structure, and beach profiles at the sides with very little reflection. The different zones were separated by wooden partitions that extended over approximately one third of the length of the wave flume. The differences in reflection coefficient between the structure and beach profiles gave rise to cross waves for a large number of regular wave tests. This phenomenon was reinforced by the presence of the pump outlet in one of sections with a beach profile. The water transport from the reservoir to the flume could not be carried out below the structure. In order not to disturb the incoming waves in the central section, the pump outlet was positioned in a side section.

Figure 7 – Photos of adapted test set-up 1

By positioning the reservoir directly behind the crest of the slope, i.e. decreasing the length of the chute, large oscillations of the water inside the reservoir occurred. Although the weigh cell measurement technique is less susceptible to such oscillations (see section 2), the output signal of the weigh cell was affected by those oscillations, enhanced by the large sampling frequency (40 Hz) of the weigh cell used during the tests. It is also worth mentioning that a pump without return valve was employed, allowing water in the outlet tube to run back to the reservoir, which impeded compensation for pumping.

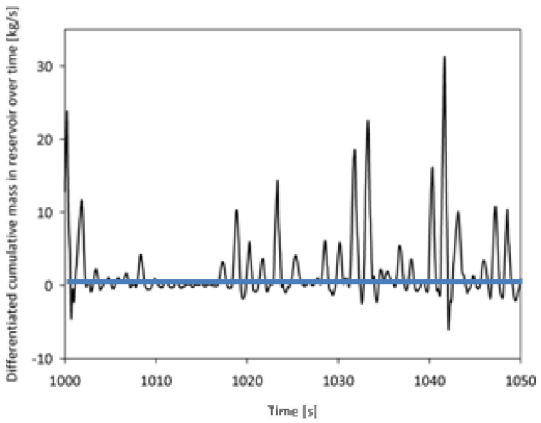

Figure 8 – Curve of differentiated cumulative mass in reservoir over time – large negative peaks occur

The "children's diseases" listed above finally give rise to the derivation of negative wave-by-wave overtopping masses. The size of the unrealistic negative peaks in the curve of the differentiated cumulative mass in the reservoir over time is a measure for the quality of determination of the wave-by-wave overtopping masses. Figure 8 shows that curve for an irregular wave test carried out with the first adapted test set-up. Negative peaks down to -7 kg/s occur, illustrating the accuracy of the measurement technique and the compensation for pumping need to be improved. A second improved test set-up was designed to meet those requirements, see section 4.

4. Adapted test set-up 2

The second adapted test set-up was installed in a wave flume with dimensions 30 m x 1 m x 1.2 m (length x width x height) at the Department of Civil Engineering of Ghent University, Belgium and used for testing during spring 2010. Compared to adapted test set-up 1, further adaptations have been carried out in order to eliminate the "children's diseases" mentioned in section 3. Figure 9 shows two drawings of the second adapted test set-up, illustrating the solutions for the "children's diseases".

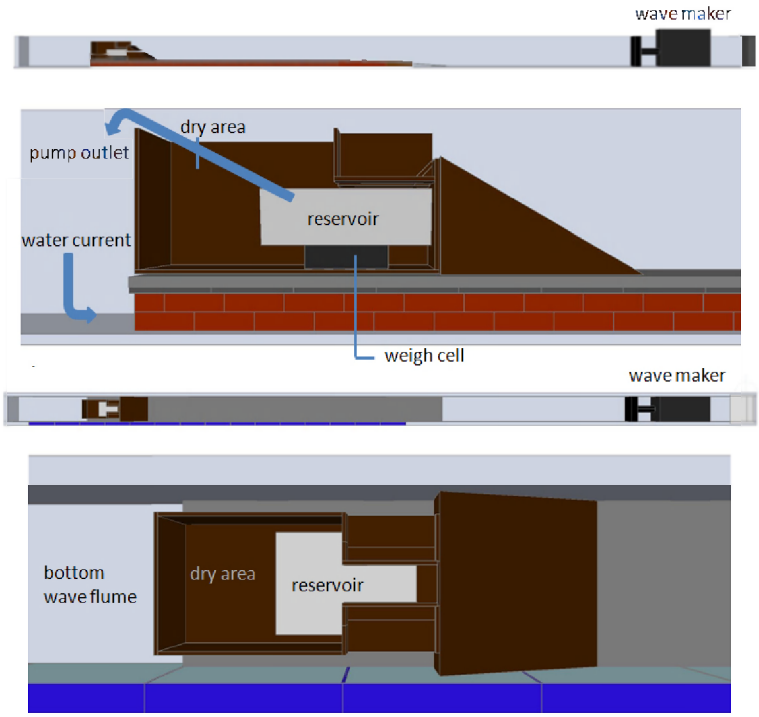

Figure 9 – Drawings of adapted test set-up 2 – side view (top) and top view (bottom)

The inability of linking the overtopping detection system signal to the size of the wave-by-wave overtopping masses has been solved by replacing the two wires of limited length by thicker wires with a length much larger than the overtopping flow depth of all overtopping waves. Figure 10 illustrates that a direct link between the height of the peaks of the overtopping detection signal and the size of the wave-by-wave overtopping masses can be made.

The shape and width of the dry area are altered in order to allow waves to overtop the structure over the whole width of the flume. The installation of beach profiles is then redundant. Furthermore, the structure is built on a hollow foreshore, which enables the water to be transported from the reservoir to the front of the wave flume below the structure, see Fig. 9. Both measures significantly reduce the generation of cross waves.

The overtopping width is reduced to 0.2 m and a smaller sampling frequency for the weigh cell (5 Hz) is applied in order to limit the effect of large oscillations on the weigh cell signal. Impact-limiting structural parts are also installed between the crest of the slope and the reservoir to decrease the oscillations of the water in the reservoir.

The final adaptations are the application of a pump with return valve and the fine-tuning of the data processing script that is used for the compensation for pumping, based on calibration tests that lead to a better understanding of the behavior of the pump during the tests.

The quality of determination of the wave-by-wave overtopping masses is again verified based on the curve of differentiated cumulative mass in the reservoir over time, see Fig. 11. Figure 11 shows that the size of the unrealistic negative peaks is significantly reduced for the second adapted test set-up, proving the positive effect of the further adaptations. This involves that a more accurate determination of the large wave-by-wave overtopping masses is achieved using the second adapted test set-up.

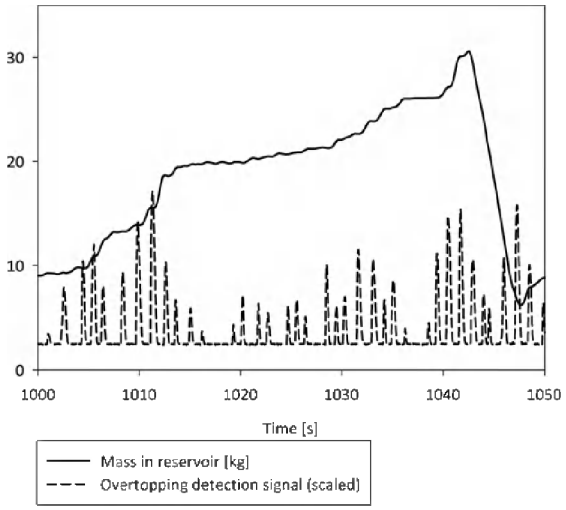

Figure 10 – Typical output of the overtopping detection system of adapted test set-up 2 with the corresponding weigh cell signal

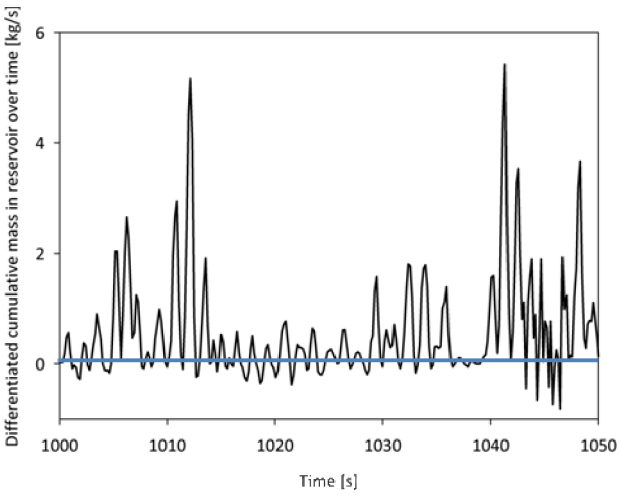

Figure 11 – Curve of differentiated cumulative mass in reservoir over time – only small negative peaks occur

5. Applications

The large wave-by-wave overtopping masses achieved with the second adapted test set-up are currently analyzed in order:

- to set up the relationship between the continuously sampled signal of the overtopping detection system and the continuously sampled wave elevations in front of the structure, and
- to determine the distribution of the wave-by-wave overtopping masses.

Concerning the distribution of the wave-by-wave overtopping masses, many references (see e.g. EurOtop (2007)) mention that those masses follow a two parameter Weibull distribution, with probability density function (pdf):

$$f(V) = \frac{b}{a}\left(\frac{V}{a}\right)^{b-1} \exp\left[-\left(\frac{V}{a}\right)^{b}\right] \qquad [2]$$

V represents the wave-by-wave overtopping volume, expressed in m³/m, while a is the scale factor of the Weibull distribution and b is the shape factor. Traditionally, for smooth impermeable sea dikes, a fixed shape factor $b = 0.75$ is used. The corresponding definition of the scale factor a is:

$$a = 0.84\, q\, T_m \frac{N_w}{N_{ow}} \qquad [3]$$

T_m represents the average wave period, q is the average overtopping rate, N_w is the number of waves during the wave record and N_{ow} is the number of overtopping waves during the wave record. The value of the shape factor above involves that only a few very large overtopping waves are responsible for most of the average overtopping rate, see e.g. EurOtop (2007). This situation is typical for sea defense structures for which small average overtopping rates occur. However, when larger overtopping takes place, the average overtopping rate will be determined by a larger number of overtopping waves. Correspondingly, the shape factor and scale factor of the Weibull distribution, defined above, possibly do not apply anymore for the case of large overtopping rates. Figure 12 shows the effect of changing the value of b for a fixed value of a = 0.102 on the pdf of a two parameter Weibull distribution.

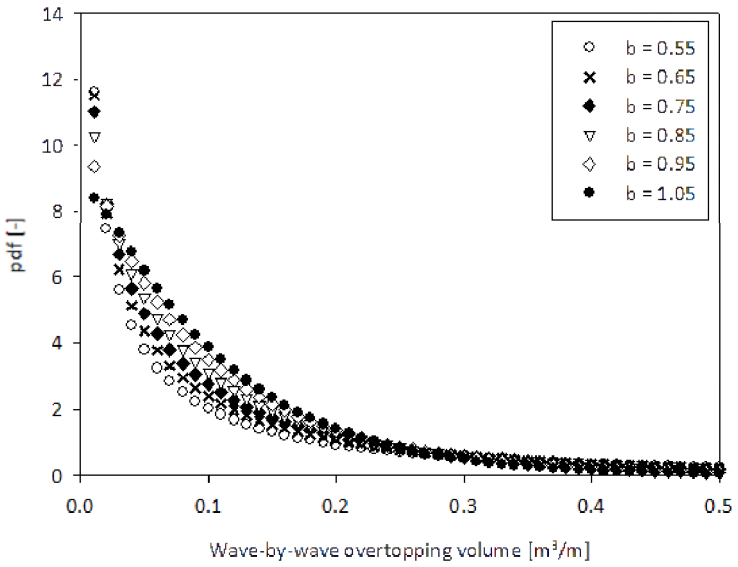

Figure 12 – Curve of probability density function corresponding to Weibull distribution with scale factor a = 0.102, for varying shape factor

By increasing the value of the shape factor, a less sharp pdf is achieved, resulting in the occurrence of a larger portion of larger overtopping volumes compared to a lower value of b. This means that for cases with large overtopping volumes, discussed in this paper, a larger value for b will have to be chosen in order to get a good agreement between the theoretical distribution and the distribution of the measured wave-by-wave overtopping volumes. Figure 13 shows a measured and predicted probability density functions for an irregular wave test with spectral wave height 0.067 m, peak wave period 1.278 s, crest freeboard 0.02 m (length scale 1/30) and slope angle 45°, using the second adapted test set-up. Two predicted probability density functions are shown: one for b = 0.75 and a calculated according to Eq. [3] (a = 0.0027) (prediction (1)); the other corresponds to b = 1.05 and a = 0.0036 (prediction (2)).

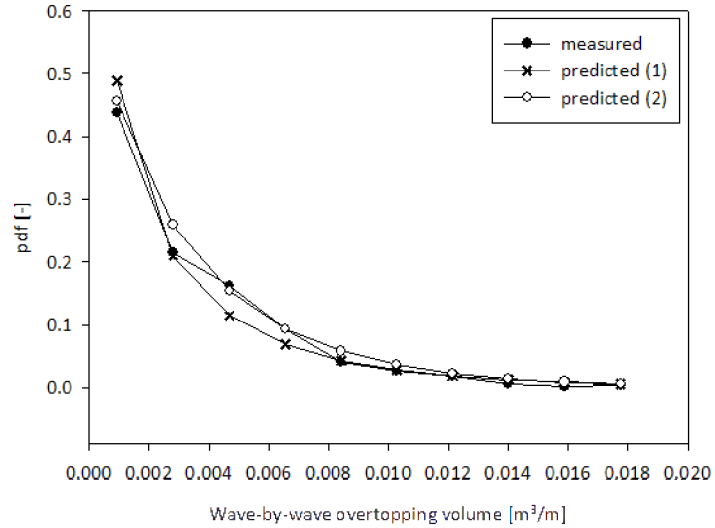

Figure 13 – Curve of probability density function corresponding to test with spectral wave height 0.067 m, peak wave period 1.278 s, crest freeboard 0.02 m (length scale 1/30) and slope angle 45°, together with predicted pdfs

Figure 13 clearly shows that the measured probability distribution is not accurately predicted by the pdf of prediction (1), which is based on the traditional definitions for scale factor a and shape factor b. The scale and shape factor of prediction (2) are chosen based on trial and error in order to have a more accurate prediction. The larger value of b for prediction (2) confirms the reasoning that was made above. Furthermore, this reveals that if the shape factor is changed, also the scale factor needs to be adapted in order to find an accurate prediction pdf.

A large number of tests have been carried out with the second adapted test set-up during 2010. The measured pdfs for all tests are currently investigated in order to determine more general expressions for a and b in Eq. [2] to give more accurate predictions of the probability density function of the wave-by-wave overtopping volumes corresponding to large average overtopping rates.

6. Conclusions

A laboratory test set-up that is able to measure large wave-by-wave overtopping masses accurately has been developed. It is based on the accurate weigh cell technique, which is traditionally used for measuring small wave overtopping masses at scale models of sea defense structures. A number of adaptations have been carried out to enable the reading of large wave-by-wave overtopping masses from the weigh cell signal. The effectiveness of those adaptations is compared through the size of the negative peaks in the curve of the differentiated cumulative mass of water in the reservoir against time. Small negative peaks are acquired by: decreasing the length of the chute, by installing a proper overtopping detection system, using a return valve for the pump, allowing wave overtopping over the whole width of the flume, guiding the outflow of the pump to the front of the wave flume below the structure, by taking a small sampling frequency for the weigh cell and by limiting the oscillations of the water inside the reservoir.

The final adapted test set-up has been used for a series of irregular wave tests, for which the distribution of the wave-by-wave overtopping masses was derived. The measured overtopping masses appear to follow a two parameter Weibull distribution with different shape and scale factors compared to the Weibull distribution corresponding to sea defense structures.

The test set-up developed in this paper can be used to measure large and small wave-by-wave overtopping masses for all types of structures.

Acknowledgments

The technicians of the Departments of Civil Engineering at Aalborg University and Ghent University are acknowledged for their help with the experimental test set-ups. The Fund for Scientific Research-Flanders (FWO-Vlaanderen) is granted for funding the research.

References

CEM, 2002. 'Coastal Engineering Manual'. Engineer Manual 1110-2-1100, U.S. Army Corps of Engineers, Washington, D.C. (in 6 volumes).

EurOtop, 2007. 'Wave Overtopping of Sea Defences and Related Structures: Assessment Manual', Environment Agency, UK/ENW Expertise Netwerk Waterkeren, NL/KFKI Kuratorium für Forschung im Küsteningenieurwesen, DE.

Kofoed, J.P., 2002. 'Wave overtopping of Marine Structures - Utilization of Wave Energy'. PhD Thesis, Aalborg University, Aalborg, DK.

Kortenhaus, A., Oumeraci, H., Geeraerts, J., De Rouck, J., Medina, J.R. and Gonzalez-Escriva, J.A., 2004a. 'Laboratory effects and other uncertainties in wave overtopping measurements', 29th International Conference on Coastal Engineering, Lisbon, P.

Lykke Andersen, T. and Burcharth, H.F., 2009. 'Three-dimensional investigations of wave overtopping on rubble mound structures'. Coastal Engineering, 56(2): 180-189.

Shin, S.-H. and Hong, K., 2005. 'Experimental study on Wave Overtopping Discharge in Sloping Structures for Wave Energy Converter', International Offshore and Polar Engineering Conference, Seoul, Korea, pp. 491-496.

Tedd, J. and Kofoed, J.P., 2009. 'Measurements of overtopping flow time series on the Wave Dragon, wave energy converter'. Renewable Energy, 34(3): 711-717.

Troch, P., Geeraerts, J., Van de Walle, B., De Rouck, J., Van Damme, L., Allsop, W. and Franco, L., 2004. 'Full-scale wave overtopping measurements on the Zeebrugge rubble mound breakwater'. Coastal Engineering, 51(7): 609-628.

Verhaeghe, H., 2005. 'Neural Network Prediction of Wave Overtopping at Coastal Structures'. PhD Thesis, Ghent University, Ghent, Belgium.